Journal of Computational Physics **179,** 1–26 (2002)
doi:10.1006/jcph.2002.7010

A Numerical Method for the Accurate Solution of the Fokker–Planck–Landau Equation in the Nonhomogeneous Case[1]

Francis Filbet* and Lorenzo Pareschi†

*IECN-INRIA project Numath—Université de Nancy I, BP 239, 54506 Vandœuvre-lès-Nancy cedex, France; and †Department of Mathematics, University of Ferrara, Via Machiavelli 35, I-44100, Ferrara, Italy and Department of Mathematics, University of Wisconsin—Madison, Van Vleck Hall, 480 Lincoln Drive, Madison, Wisconsin 53706
E-mail: filbet@iecn.u-nancy.fr and pareschi@dm.unife.it

Received April 3, 2001; revised January 25, 2002

A new approach for the accurate numerical solution of the Fokker–Planck–Landau (FPL) equation in the nonhomogeneous case is presented. The method couples, through a time-splitting algorithm, a finite-volume scheme for the transport with a fast spectral solver for the efficient solution of the collision operator recently introduced. The scheme allows the use of different grids in the velocity space for the transport and the collision phases. The use of a suitable explicit Runge–Kutta solver for the time integration of the collision phase permits avoid once of excessive small time steps induced by the stiffness of the diffusive collision operator. Numerical results for both space homogeneous and space nonhomogeneous situations show the efficiency and the accuracy of the present method.

Key Words: Fokker–Planck–Landau equation; Vlasov–Poisson system; spectral methods; splitting algorithms.

1. INTRODUCTION

The Landau or Fokker–Planck–Landau (FPL) equation is a common kinetic model used to describe long-range interactions between charged particles in plasma physics, accelerator physics, and astrophysics. Coulomb collisions are essentially important in a great variety of applications, ranging from laser and particle beam interactions with plasma [11, 42], to shock waves and plasma expansion, to superthermal radiation [24] and ion transport in fusion reactors [31].

[1] Research supported by the TMR project "Asymptotic Methods in Kinetic Theory," Contract ERB FMRX CT97 0157.

0021-9991/02 $35.00

The model is described by a nonlinear partial integrodifferential equation of the form

$$\frac{\partial f}{\partial t} + v \cdot \nabla_x f + E(t,x) \cdot \nabla_v f = \frac{1}{\varepsilon} Q(f,f), \quad v \in \mathbb{R}^3,\ x \in \Omega \subset \mathbb{R}^3, \tag{1}$$

where the unknown distribution function $f(t,x,v)$ depends on time t, position x, and velocity v of particles. In (1) ε is the Knudsen number, $F(t,x)$ the force field given by the solution of a normalized Poisson equation

$$E(t,x) = -\nabla_x \phi(t,x), \quad -\Delta_x \phi(t,x) = \int_{\mathbb{R}^3} f(t,x,v)\, dv, \tag{2}$$

and $Q(f,f)$ a collision operator acting on v only:

$$Q(f,f)(v) = \nabla_v \cdot \int_{\mathbb{R}^3} \Phi(v-v^*)[\nabla_v f(v) f(v^*) - \nabla_{v^*} f(v^*) f(v)]\, dv^*. \tag{3}$$

In the collision operator the dependence of f from (x,t) has been omitted for simplicity and Φ is a 3×3 nonnegative and symmetric matrix that depends on the interaction between particles of the form

$$\Phi(v) = |v|^{\gamma+2} S(v), \quad \gamma \in \mathbb{R} \quad \text{and} \quad S(v) = Id - \frac{v \otimes v}{|v|^2}. \tag{4}$$

Different values of γ lead to the usual classification in hard potentials $\gamma > 0$, Maxwellian molecules $\gamma = 0$, or soft potentials $\gamma < 0$. This latter case involves the Coulombian case $\gamma = -3$, which is of primary importance for applications.

In order to define completely the mathematical problem for Eq. (1) suitable boundary conditions on $\partial\Omega$ should be considered. Apart from ingoing/outgoing particle flows the most widely used boundary conditions to describe the interactions of particles with a solid surface are the specular reflecting and the diffusive ones, or a linear combination of them usually referred to as Maxwell's boundary conditions [13].

The algebraic structure of the FPL operator is similar to the Boltzmann one; this leads to physical properties such as the conservation of mass, momentum, and energy,

$$\int_{\mathbb{R}^3} Q(f,f)(v) \begin{pmatrix} 1 \\ v \\ |v|^2 \end{pmatrix} dv = 0,$$

and the decay of the kinetic entropy $H(t)$,

$$\frac{dH}{dt}(t) = \frac{d}{dt} \int_{\mathbb{R}^3} f(t,v) \ln(f(t,v))\, dv \le 0.$$

This implies that the equilibrium states of the FPL operator, i.e., the functions satisfying $Q(f,f) = 0$, are given by Maxwellians

$$M_{\rho,u_0,T}(v) = \frac{\rho}{(2\pi k_B T)^{3/2}} \exp\left(-\frac{|v-u|^2}{2k_B T}\right),$$

where k_B is Boltzmann's constant, ρ the total mass, u the mean velocity, and T the temperature of the plasma given by

$$\rho = \int_{\mathbb{R}^3} f(v)\,dv, \quad u = \frac{1}{\rho}\int_{\mathbb{R}^3} f(v)v\,dv, \quad T = \frac{1}{3\rho}\int_{\mathbb{R}^3} f(v)(u-v)^2\,dv.$$

Classically the collision operator (3) is obtained as a remedy to the loss of finiteness of the Boltzmann collision operator for Coulomb interactions. In Coulomb collisions small-angle collisions play a more important role than collision resulting in large velocity changes. The original derivation of the equation based on this idea is due to Landau [25]. Depending on one's taste and notion of rigor, several mathematical derivations of the equations have been performed; we mention here the works of Arsen'ev and Buryak [1], Degond and Lucquin-Desreux [16], Desvillettes [18], and Rosenbluth *et al.* [43]. For a recent review of the main mathematical aspects related to the equation we refer the reader to Villani [47] (and the references therein).

In contrast with the Boltzmann equation, where Monte Carlo methods play a major role in numerical simulations and their connection with the Boltzmann equation has been widely studied (see [14] for a review about rigorous mathematical results on simulation methods), the extension of these methods to long-range forces, in particular Coulomb interactions, is challenging and has not yet been completely successful. Most of the particle methods for Coulomb interaction, although extensively used, have been derived more on a physical intuition basis and not directly from the Landau equation. A detailed discussion about this is beyond the aims of the present paper and we refer the reader to [4, 32] for a more complete treatment and a recent review.

Several deterministic numerical approaches have been considered to Fokker–Planck-type equations [2, 5, 7–9, 15, 17, 20, 21, 26, 27, 29, 41, 46]. Most of them are based on finite differences and are devoted to the simpler diffusive Fokker–Planck model. Only in the recent years has a considerable amount of attention been directed toward the full Landau equation. Due to the computational complexity of the equation (essentially caused by the large number of variables and the threefold collision integral) many papers have been devoted to treating simpler space homogeneous situations (the distribution function f does not depend on x) in the isotropic case [5] or to cylindrically symmetric problems [40]. The construction of conservative and entropic schemes for the space homogeneous case has been proposed by Degond and Lucquin-Desreux [17] and Buet and Cordier [7, 8]. These schemes are built in such a way that the main physical properties are conserved at a discrete level. Positivity of the solution and discrete entropy inequality are also satisfied. Unfortunately, the direct implementation of such schemes for space nonhomogeneous computations is very expensive since the computational cost increases roughly in proportion to the square of the number of parameters used to represent the distribution function in the velocity space.

Thus several fast approximated algorithms to reduce the computational complexity of these methods, based on multipole expansions [26] or multigrid techniques [8], have been proposed. Although these fast schemes are able to preserve the most relevant physical properties, the range of applications seems limited and the degree of accuracy of such approaches has not been studied. A different approach, based on spectral methods, has been recently proposed for the Boltzmann [34, 35] and FPL [37, 38] collision operators. In the case of (3)

the spectral scheme permits obtainment of spectrally accurate solutions with a reduction in the quadratic cost N^2 to $N \log_2 N$, where N is the total number of unknowns in the velocity space. The lack of discrete conservations in the spectral scheme (mass is preserved, whereas momentum and energy are approximated with spectral accuracy) is compensated for by its higher accuracy and efficiency. In particular the scheme allows easily the implementation of grid-refinement techniques in the velocity space. A detailed comparison of the spectral scheme with the schemes proposed in [9, 26] has been done [10]. We mention here also a similar approach by Bobylev and Rijasanow for the Boltzmann equation in the Maxwellian case [6].

Most of these methods have proved their efficiency in the homogeneous case, but to the best of our knowledge, they have not been extended to the nonhomogeneous situation. The main goal of this paper is to develop a scheme for the full Fokker–Planck–Landau equation by coupling the fast spectral technique for (3) with a flux conservative method based on the characteristic curves for the transport step [22, 44] through a splitting algorithm. In the coupling procedure a suitably explicit Runge–Kutta solver for the time integration of the collision phases [30] permits avoidance of the small time steps induced by the stiffness of the diffusive collision operator.

The main properties of our method are here summarized:

- Spectrally accurate evaluation of $Q(f, f)$ with $O(N \log_2 N)$ operations.
- Second-order accuracy in time, avoiding excessive small time-step restrictions caused by the diffusive stiffness of the collision operator.
- Third-order accuracy in both velocity and physical space during transport.
- The possibility of using different grids in the velocity space for the transport and the collision phases.

In addition, thanks to the splitting strategy, the resulting scheme is highly parallelizable. The aforementioned properties, as we see, are essential to performing efficiently space nonhomogeneous computations with great accuracy.

The rest of the article is organized as follows. In the next section we describe the main features of our numerical methods. First we derive the fast spectral method for the approximation of the collision operator. Next the flux conservative scheme for the transport part and the discretization of boundary conditions are discussed. Finally, several numerical tests for three-dimensional space homogeneous problems and two-dimensional space nonhomogeneous problems are presented.

2. THE NUMERICAL METHOD

As is usually done for a kinetic equation like (1) a simple first-order time splitting is obtained considering in a small time interval $\Delta t = [t^n, t^{n+1}]$, the numerical solution of the space homogeneous collision phase $S_2^n(f, \Delta t)$,

$$\begin{cases} \dfrac{\partial f^*}{\partial t} = \dfrac{1}{\varepsilon} Q(f^*, f^*), \\ f^*(0, x, v) = f^n(x, v), \end{cases} \tag{5}$$

and the transport step $S_1^n(f, \Delta t)$,

$$\begin{cases} \dfrac{\partial f^{**}}{\partial t} + v \cdot \nabla_x f^{**} + F(t,x) \cdot \nabla_v f^{**} = 0, \\ f^{**}(0,x,v) = f^*(\Delta t, x, v). \end{cases} \tag{6}$$

The approximated value at time t^{n+1} is then given by

$$f^{n+1}(x,v) = f^{**}(\Delta t, x, v) = S_1^n(\Delta t) \circ S_2^n(\Delta t). \tag{7}$$

A second-order scheme for moderately stiff problems can be easily derived simply by symmetrizing the first-order scheme [45],

$$f^{n+1} = S_1^n(f, \Delta t/2) \circ S_2^n(f, \Delta t) \circ S_1^n(f, \Delta t/2), \tag{8}$$

provided every step is solved with a method at least second-order accurate in time. Recently second-order splitting algorithms for Boltzmann-like equations were presented in [33].

Clearly the crucial point is the numerical solution to (5) because of the presence of the collision operator. In the following, we first present the numerical approximation of the collision operator using a spectral method and show how the resulting discretization can be computed with fast algorithms. Then we discuss some issues related to the time discretization of the collision phase. Finally we describe the scheme for the transport step and the discretization of boundary conditions.

2.1. A Fast Spectral Method for the Collision Step

This method has been recently proposed to approximate Boltzmann [35] and Fokker–Planck–Landau [37] equations. Here we recall briefly the main derivation of the method and refer to the previous references for the mathematical properties of this approximation (consistency and spectral accuracy).

Let us write the operator on the usual form,

$$Q(f,f) = \nabla_v \cdot \int_{\mathbb{R}^d} \Phi(v - v^*)[(\nabla_v f(t,v)) f(t,v^*) - (\nabla_{v^*} f(t,v^*)) f(t,v)]\, dv^*,$$

where d is the dimension of the velocity space.

For simplicity, we will assume that the support of the distribution function is included in the ball $B(0, R/2)$, with $R > 0$, and also that the collision integral is compactly supported in the ball $B(0, R)$. This assumption is clearly false in general, but it is essential from a numerical point of view for any method that uses a finite-velocity space for the representation of the distribution function. This is equivalent to assuming that the distribution function is truncated to zero for large velocities $|v| > R$.

We approximate the distribution using a partial sum of a Fourier series,

$$f_N(t,v) = \sum_{k \in \{-N,\dots,N\}} \hat{f}_k(t) e^{i \frac{\pi}{R} k \cdot v}, \tag{9}$$

where $k \in \mathbb{Z}^d$, $N = (n, \dots, n)$ is a multiinteger, n is the number of half modes in each direction, and the kth mode is given by

$$\hat{f}_k(t) = \frac{1}{(2R)^d} \int_{B(0,R)} f(t, v) e^{-i\, k\cdot v}\, dv.$$

Then, substituting the approximation $f_N(t, v)$ in operator (1), we obtain the expression

$$Q(f_N, f_N) = \left[\frac{\pi}{R}\right]^{\gamma+d} \sum_{l,m\in\{-N,\dots,N\}} \hat{f}_l(t)\hat{f}_m(t)\hat{\beta}_L(l, m) e^{i\frac{\pi}{R}(l+m)\cdot v}, \tag{10}$$

where $\hat{\beta}_L(l, m)$ reads (using a simple change of variable)

$$\begin{aligned}\hat{\beta}_L(l, m) &= \int_{B(0,\pi)} |w|^{\gamma+2} \left[(l+m)(l-m) - (l+m)\cdot\frac{w}{|w|}(l-m)\cdot\frac{w}{|w|}\right] e^{i w\cdot m}\, dw \\ &= (\hat{B}(l, m) - \hat{B}(m, m))\end{aligned}$$

with

$$\hat{B}(l, m) = \int_{B(0,\pi)} |w|^{\gamma+2} \left[l^2 - \left(l\cdot\frac{w}{|w|}\right)^2\right] e^{i w\cdot m}\, dw.$$

Now projecting $Q(f_N, f_N)$ back to the space of trigonometric polynomials of degree $\le n$ [12, 23], we get the following system of differential equations:

$$\frac{d\hat{f}_k}{dt} = \frac{1}{\varepsilon}\left[\frac{\pi}{R}\right]^{\gamma+d} \sum_{\substack{l,\, m\in\{-N,\dots,N\}\\ l+m=k}} \hat{f}_l\hat{f}_m[\hat{B}(l, m) - \hat{B}(m, m)], \quad k \in \{-N, \dots, N\}. \tag{11}$$

To define a numerical algorithm we must compute the quantities $\hat{B}(l, m)$. The computation can be split into two parts:

$$\begin{aligned}\hat{B}(l, m) &= \int_{B(0,\pi)} |w|^{\gamma+2} \left[l^2 - \left(l\cdot\frac{w}{|w|}\right)^2\right] e^{i w\cdot m}\, dw, \\ &= l^2 \int_{B(0,\pi)} |w|^{\gamma+2} e^{i w\cdot m}\, dw - \sum_{i,j=1}^{3} l_i l_j \int_{B(0,\pi)} |w|^{\gamma+2} \frac{w_i w_j}{|w|^2} e^{i w\cdot m}\, dw.\end{aligned}$$

Now setting

$$\begin{aligned}F_1(m) &= \int_{B(0,\pi)} |w|^{\gamma+2} \left(1 - \frac{(m\cdot g)^2}{|m|^2|g|^2}\right) e^{i w\cdot m}\, dw, \\ F_2(m) &= \int_{B(0,\pi)} |w|^{\gamma+2} e^{i w\cdot m}\, dw, \\ I_{i,j}(m) &= \int_{B(0,\pi)} |w|^{\gamma+2} \frac{w_i w_j}{|w|^2} e^{i w\cdot m}\, dw,\end{aligned}$$

we obtain the ODE system

$$\frac{d\hat{f}_k}{dt} = \frac{1}{\varepsilon}\left[\frac{\pi}{R}\right]^{\gamma+d} \sum_{m\in\{-N,\dots,N\}} \hat{f}_{k-m}\hat{f}_m[(k-m)^2F_2(m) - m^2F_1(m)]$$
$$- \frac{1}{\varepsilon}\left[\frac{\pi}{R}\right]^{\gamma+d} \sum_{i,j=1}^{d} \sum_{m\in\{-N,\dots,N\}} \hat{f}_{k-m}\hat{f}_m(k_i - m_i)(k_j - m_j)I_{i,j}(m). \quad (12)$$

The coefficients $F_1(m)$, $F_2(m)$, and $I_{i,j}$ depend only on γ and require the computation of simple one-dimensional integrals. Thus they can be approximated very accurately and stored in suitable matrices once and for all. Further details can be found in [37, 38].

Finally, to approximate the right hand side of the system, we only have to compute several discrete convolution sums of the form

$$\forall k \in \{-N, \dots, N\}, \quad S_k = \sum_{m\in\{-N,\dots,N\}} g_m h_{k-m}.$$

This can be efficiently done using transform methods [12]. The following is an $O((2n)^d \log_2((2n)^d))$ algorithm based on the fast Fourier transform (FFT):

- Apply the FFT method to transform g_m and h_{k-m} into $\hat{g}_m$ and $\hat{h}_{k-m}$ with a cost $O((2n)^d \log_2(2n)^d)$.
- Compute the sum in the Fourier space with a cost $O((2n)^d)$.
- Apply the inverse FFT to obtain the final result with a cost $O((2n)^d \log_2(2n)^d)$.

Let now $\mathcal{P}_N : L^2([-\pi,\pi]^d) \to \mathbb{P}^N$ be the orthogonal projection upon the space of trigonometric polynomials of degree N in v, $\mathbb{P}^N$ in the inner product of $L^2([-\pi,\pi]^d)$. Then the spectral method can be written in equivalent form as

$$\frac{\partial f_N}{\partial t} = Q_N(f_N, f_N),$$

with initial data $f_N(v, t=0) = f_{0,N}(v)$ and

$$Q_N(f_N, f_N) := \mathcal{P}_N Q(f_N, f_N), \quad (13)$$

where $Q(f_N, f_N)$ is given by (10).

It is easy to verify that the spectral method preserves mass whereas variations of momentum and energy are controlled by the spectral accuracy [35, 37].

THEOREM 2.1. *The spectral approximation of the collision operator defined by* (13)–(10) *is such that the following properties hold.*

(i) (Consistency) *Let* $f \in H^2_p([-\pi,\pi]^d)$, *then* $\forall r \geq 0$,

$$\|Q(f,f) - Q_N(f_N, f_N)\|_2 \leq C\left(\|f - f_N\|_{H^2_p} + \frac{\|Q(f_N, f_N)\|_{H^r_p}}{N^r}\right),$$

where C *depends on* $\|f\|_2$.

(ii) (Spectral accuracy) *Let* $f \in H_p^r([-\pi, \pi]^d)$, $r \geq 2$, *then*

$$\|Q(f, f) - Q_N(f_N, f_N)\|_2 \leq \frac{C}{N^{r-2}}\left(\|f\|_{H_p^r} + \|Q(f_N, f_N)\|_{H_p^r}\right).$$

In the previous theorem H_p^r denotes the Sobolev space of periodic functions up to the rth-order derivative over $[-\pi, \pi]^d$. No information is available on the discrete equilibrium states, the decay of the numerical entropy, and the preservation of positivity. We mention that conservative schemes based on similar spectral techniques have been developed in [6, 34]. Positive schemes have been constructed in [36]. However the numerical results obtained with these schemes denoted a strong loss of accuracy in the results when compared to the original spectral method.

2.2. The Fully Discrete Scheme

In order to obtain a fully discrete scheme we have to deal with the time discretization of (12). The strong nonlinearity of the system of equations and the large number of unknowns makes prohibitively expensive the use of an implicit (and hence iterative) scheme to discretize the resulting ODE system. We refer to [31] for some results in this direction. On the other hand the use of explicit methods, due to the diffusive structure of the collision operator, which leads to the solving of a stiff problem, gives a stability condition which forces the time step to be on the order of the square of the velocity step.

Here we refer to the definition of stability used by Lebedev [28]. Consider the following Cauchy problem for ordinary differential equations.

$$\frac{dU}{dt} = f(t, U(t)), \quad U(0) = U_0,$$

with $U \in \mathbb{R}^m$.

Let

$$J_{ij} = \left(\frac{\partial f_i}{\partial U_j}\right)$$

be the Jacobian matrix. First let the spectrum of J be real and let λ be an upper bound of the modulo of the negative eigenvalues of the Jacobian matrix; then for an explicit Euler scheme the stability condition on the time step is given by

$$\lambda \Delta t < 1.$$

This is stated by the following.

PROPOSITION 2.1. *Let* $\hat{f}_k^{n+1}$ *be the approximation of the kth mode at time* $t^{n+1} = (n+1)\Delta t$, *using the spectral method coupled with the explicit Euler scheme. Then, the times step* Δt *has to satisfy the following stability condition,*

$$\exists C(\gamma, d, f) > 0, \quad \Delta t \leq C(\gamma, d, f)\frac{\varepsilon}{N^2},$$

where $N^2 = dn^2$ *and n is the number of modes in each direction.*

Proof. Let us set $FP_k(\hat{f})$ such that

$$FP_k(\hat{f}) = \frac{1}{\varepsilon}\left[\frac{\pi}{R}\right]^{\gamma+d} \sum_{m\in\{-N,\dots,N\}} \hat{f}_{k-m}\hat{f}_m[(k-m)^2F_2(m) - m^2F_1(m)]$$
$$- \frac{1}{\varepsilon}\left[\frac{\pi}{R}\right]^{\gamma+d} \sum_{i,j=1}^{d} \sum_{m\in\{-N,\dots,N\}} \hat{f}_{k-m}\hat{f}_m(k_i - m_i)(k_j - m_j)I_{i,j}(m).$$

Then, using an explicit first-order Euler scheme, we get

$$\forall k \in \{-N,\dots,N\}, \quad \hat{f}_k^{n+1} = \hat{f}_k^n + \Delta t\ FP_k(\hat{f}^n),$$

and the stability condition on the time step is given by

$$\forall k \in \{-N,\dots,N\}, \quad \Delta t \le 1/Lip(FP_k(.)),$$

where $Lip(FP_k(\cdot))$ is the Lipschitz constant of $FP_k(\cdot)$, which can be evaluated by computing the Jacobian $\mathcal{J}_{k,l}$. Then, there exists a positive constant $C(\gamma, d, f) > 0$, such that

$$|\mathcal{J}_{k,l}| = \left|\frac{d}{dg_l}FP_k(\hat{f}^n)\right|$$
$$\le \frac{C(\gamma,d,f)}{\varepsilon}\max\left(\hat{f}_{k-l}^n, \hat{f}_l^n\right)\Big[|k-l|^2(|F_2(l)| + F_1(k-l)|)$$
$$+\ l^2(|F_1(l)| + F_2(k-l)|) + \sum_{i,j=1}^{d}|k-l|^2|I_{i,j}(l)| + |l|^2|I_{i,j}(k-l)|\Big].$$

But, the coefficients $F_1(m)$, $F_2(m)$, and $I_{i,j}$ are uniformly bounded:

$$|F_1(m)|,\ |F_2(m)|,\ |I_{i,j}(m)| \le 2\frac{\pi^{\gamma+2+d}}{\gamma+2+d}.$$

Thus we have

$$|\mathcal{J}_{k,l}| = \left|\frac{dFP_k}{dg_l}(\hat{f}^n)\right| \le \frac{C(\gamma,d,f)}{\varepsilon}\hat{f}_0^n N^2.$$

Finally, the time step is bounded by

$$\Delta t \le 1/Lip(FP_k(\hat{f}^n)) \le \varepsilon/\left(C(\gamma,d,f)\hat{f}_0^n\ N^2\right) \quad \forall k \in \{-N,\dots,N\}. \qquad \square$$

As expected, from Proposition 2.1, the time step is decreasing when the number of modes increases or when the Knudsen number goes to zero. This drawback can be partially avoided using a high-order explicit scheme with a large stability interval. In our numerical code we have adopted the third-order DUMKA scheme proposed recently by Medovikov [30]. The method is a composite Runge–Kutta method derived from its stability polynomials computed in such a way that the stability domain is optimal. This is achieved in two steps. The first is to compute the stability polynomial of a given order with optimal stability

domains, i.e., to possess a Chebyshev alternation. Roots of these polynomials are computed numerically. Then the corresponding explicit Runge–Kutta method is realized with the help of the theory of composition methods. This method, thanks to the large stability domain, allows reasonable stiffness and, thanks to the explicitness, does not increase the computational complexity of the final algorithm. The efficiency of the method can be strongly improved using an adaptive time-stepping procedure.

2.3. Discretization of the Transport Step

In this section, we discuss the numerical resolution of the Vlasov equation, which characterizes the transport step. To this aim we use an Eulerian method which consists of discretizing the distribution function f on a phase space grid.

Let us consider the Vlasov equation written in the form

$$\frac{\partial f}{\partial t} + \mathrm{div}_x(v\, f) + \mathrm{div}_v(F(t,x) f) = 0 \tag{14}$$

coupled with the normalized Poisson equation,

$$F(t,x) = -\nabla_x \phi(t,x), \quad -\Delta_x \phi(t,x) = \int_{\mathbb{R}^d} f(t,x,v)\, dv. \tag{15}$$

The time discretization is based on the following splitting algorithm on $\Delta t = [t^n, t^{n+1}]$.

1. Solve a free transport equation on $\Delta t/2$,

$$\begin{cases} \dfrac{\partial f^{(1)}}{\partial t} + \mathrm{div}_x\left(v f^{(1)}\right) = 0, \\ f^{(1)}(0,x,v) = f^n(x,v). \end{cases} \tag{16}$$

2. Compute the electric field F at time $t^{n+1/2}$ by substituting $f^{(1)}(\Delta t/2, x, v)$ in the Poisson equation and solve on Δt the equation

$$\begin{cases} \dfrac{\partial f^{(2)}}{\partial t} + \mathrm{div}_v\left(F\left(t^{n+1/2}, x\right) f^{(2)}\right) = 0, \\ f^{(2)}(0,x,v) = f^{(1)}(\Delta t/2, x, v). \end{cases} \tag{17}$$

3. Solve a free transport equation on $\Delta t/2$,

$$\begin{cases} \dfrac{\partial f^{(3)}}{\partial t} + \mathrm{div}_x\left(v f^{(3)}\right) = 0, \\ f^{(3)}(0,x,v) = f^{(2)}(\Delta t/2, x, v), \end{cases} \tag{18}$$

and set $f(t^{n+1}, x, v) = f^{(3)}(\Delta t, x, v)$.

As for Strang splitting [45] a second-order-accurate solution of every step guarantees second-order accuracy of the procedure. Using this time splitting, we can restrict ourselves, without loss of generality, to the discretization of the one-dimensional transport equation

$$\partial_t f + \partial_x(u\, f) = 0, \quad \forall (t,x) \in \mathbb{R}^+ \times [x_{min}, x_{max}], \tag{19}$$

where u is a constant velocity. Then, the solution of the transport equation at time t^{n+1} reads

$$f(t^{n+1}, x) = f(t^n, x - u\Delta t), \quad \forall x \in [x_{min}, x_{max}].$$

Now, let us introduce a finite set of mesh points $\{x_{i+1/2}\}_{i\in I}$ on the computational domain $[x_{min}, x_{max}]$. We will use the notations $\Delta x = x_{i+1/2} - x_{i-1/2}$ and $C_i = [x_{i-1/2}, x_{i+1/2}]$. Assuming the values of the distribution function are known at time $t^n = n\Delta t$, we compute the new values at time t^{n+1} by integration of the distribution function on each subinterval. Thus, using the explicit expression of the solution, we have

$$\int_{x_{i-1/2}}^{x_{i+1/2}} f(t^{n+1}, x)\, dx = \int_{x_{i-1/2}-u\Delta t}^{x_{i+1/2}-u\Delta t} f(t^n, x)\, dx;$$

then, setting

$$\Phi_{i+1/2}(t^n) = \int_{x_{i+1/2}-u\Delta t}^{x_{i+1/2}} f(t^n, x)\, dx,$$

we obtain the conservative form

$$\int_{x_{i-1/2}}^{x_{i+1/2}} f(t^{n+1}, x)\, dx = \int_{x_{i-1/2}}^{x_{i+1/2}} f(t^n, x)\, dx + \Phi_{i-1/2}(t^n) - \Phi_{i+1/2}(t^n). \tag{20}$$

The evaluation of the average of the solution over $[x_{i-1/2}, x_{i+1/2}]$ allows us to ignore fine details of the exact solution, which may be costly to compute. The main step is now to choose an efficient method to reconstruct the distribution function from the values of each cell C_i. In [22], the author used simple linear interpolation. Unfortunately this approach does not give a positive scheme and does not control spurious oscillations. Here, we consider a reconstruction via a primitive function. Let $F(t^n, x)$ be a primitive of the distribution function $f(t^n, x)$. If we denote by

$$f_i^n = \frac{1}{\Delta x} \int_{x_{i-1/2}}^{x_{i+1/2}} f(t^n, x)\, dx,$$

then $F(t^n, x_{i+1/2}) - F(t^n, x_{i-1/2}) = \Delta x f_i^n$ and

$$F\left(t^n, x_{i+1/2}\right) = \Delta x \sum_{k=0}^{i} f_k^n = w_i^n.$$

In the sequel, the time variable t^n only acts as a parameter and will be omitted. A reconstruction method allowing us to preserve positivity and maximum principle can be obtained using slope correctors. We build a first approximation of the primitive on the interval $[x_{i-1/2}, x_{i+1/2}]$ using the stencil $\{x_{i-3/2}, x_{i-1/2}, x_{i+1/2}, x_{i+3/2}\}_{i\in I}$,

$$\begin{aligned}\tilde{F}_h(x) = w_{i-1} &+ \left(x - x_{i-1/2}\right) f_i + \frac{1}{2\Delta x}\left(x - x_{i-1/2}\right)\left(x - x_{i+1/2}\right)[f_{i+1} - f_i] \\ &+ \frac{1}{6\Delta x^2}\left(x - x_{i-1/2}\right)\left(x - x_{i+1/2}\right)\left(x - x_{i+3/2}\right)[f_{i+1} - 2f_i + f_{i-1}],\end{aligned}$$

where we used the relation $w_i - w_{i-1} = \Delta x f_i$. Thus, by differentiation, we obtain a third-order-accurate approximation of the distribution function on the interval $[x_{i-1/2}, x_{i+1/2}]$:

$$\begin{aligned}\tilde{f}_h(x) &= \frac{d\tilde{F}_h}{dx}(x)\\ &= f_i + \frac{1}{6\Delta x^2}\big[2(x-x_i)\big(x-x_{i-3/2}\big) + \big(x-x_{i-1/2}\big)\big(x-x_{i+1/2}\big)\big](f_{i+1}-f_i)\\ &\quad + \frac{1}{6\Delta x^2}\big[2(x-x_i)\big(x-x_{i+3/2}\big) + \big(x-x_{i-1/2}\big)\big(x-x_{i+1/2}\big)\big](f_i-f_{i-1}).\end{aligned}$$

In order to satisfy a maximum principle and to avoid spurious oscillations we introduce the slope correctors

$$\begin{aligned}f_h(x) &= f_i + \frac{\epsilon_i^+}{6\Delta x^2}\big[2(x-x_i)\big(x-x_{i-3/2}\big) + \big(x-x_{i-1/2}\big)\big(x-x_{i+1/2}\big)\big](f_{i+1}-f_i)\\ &\quad + \frac{\epsilon_i^-}{6\Delta x^2}\big[2(x-x_i)\big(x-x_{i+3/2}\big) + \big(x-x_{i-1/2}\big)\big(x-x_{i+1/2}\big)\big](f_i-f_{i-1}),\end{aligned} \tag{21}$$

with

$$\epsilon_i^{\pm} = \begin{cases} \min(1; 2f_i/(f_{i\pm1}-f_i)) & \text{if } f_{i\pm1}-f_i > 0,\\ \min(1; -2(f_\infty - f_i)/(f_{i\pm1}-f_i)) & \text{if } f_{i\pm1}-f_i < 0,\end{cases} \tag{22}$$

where $f_\infty = \max_{j\in I}\{f_j\}$. We have the following.

PROPOSITION 2.2. *The approximation of the distribution function $f_h(x)$ defined by* (21)–(22) *satisfies the following.*

(i) (Conservation of the average) *For all $i \in I$, $\int_{x_{i-1/2}}^{x_{i+1/2}} f_h(x)\,dx = \Delta x f_i$.*
(ii) (Maximum principle) *For all $x \in (x_{min}, x_{max})$, $0 \le f_h(x) \le f_\infty$.*

Proof. Let us consider $x \in C_i = [x_{i-1/2}, x_{i+1/2}]$ and denote by

$$\begin{aligned}\alpha(x) &= \frac{1}{\Delta x^2}\big[2(x-x_i)\big(x-x_{i-3/2}\big) + \big(x-x_{i-1/2}\big)\big(x-x_{i+1/2}\big)\big],\\ \beta(x) &= \frac{1}{\Delta x^2}\big[2(x-x_i)\big(x-x_{i+3/2}\big) + \big(x-x_{i-1/2}\big)\big(x-x_{i+1/2}\big)\big].\end{aligned}$$

It is easy to check that

$$\int_{x_{i-1/2}}^{x_{i+1/2}} \alpha(x)\,dx = \int_{x_{i-1/2}}^{x_{i+1/2}} \beta(x)\,dx = 0;$$

then the conservation of the average immediately follows. To obtain the preservation of positivity, assuming the values $\{f_j\}_{j\in I}$ are positive, we observe that in the cell C_i, the function $\alpha(x)$ increases whereas $\beta(x)$ decreases, and $\alpha(x), \beta(x) \in [-1, 2]$. We split $f_h(x)$ as the sum of $h(x)$ and $g(x)$ with

$$h(x) = \frac{1}{3}\left[f_i + \frac{\alpha(x)}{2}\epsilon_i^+(f_{i+1}-f_i)\right], \quad g(x) = \frac{1}{3}\left[2f_i + \frac{\beta(x)}{2}\epsilon_i^-(f_i-f_{i-1})\right].$$

The function $h(x)$ (resp. $g(x)$) is a combination of f_i and f_{i+1} (resp. f_{i-1} and f_i); then from the value of ϵ_i^+ (resp. ϵ_i^-), it is easy to prove that $h(x)$ (resp. $g(x)$) is positive. Using a similar decomposition, we also prove that $f_h(x)$ is bounded by f_∞. □

From this reconstruction, we approximate the quantity $\Phi_{i+1/2}(t^n)$ by looking for the cell C_j such that $x_{i+1/2} - u\Delta t \in C_j$ and setting $\alpha_i = x_{j+1/2} - (x_{i+1/2} - u\Delta t)$. Then for a positive propagating velocity u, we get the following scheme:

$$\begin{aligned}\Phi_{i+1/2}(t^n) &= \int_{x_{j+1/2}-\alpha_i}^{x_{i+1/2}} f(t^n, x)\,dx \\ &= \Delta x \sum_{k=j+1}^{i} f_k + \alpha_i \Bigg[f_i + \frac{\epsilon_j^+}{6}\left(1 - \frac{\alpha_i}{\Delta x}\right)\left(2 - \frac{\alpha_i}{\Delta x}\right)(f_{j+1} - f_j) \\ &\quad + \frac{\epsilon_j^-}{6}\left(1 - \frac{\alpha_i}{\Delta x}\right)\left(1 + \frac{\alpha_i}{\Delta x}\right)(f_j - f_{j-1}) \Bigg].\end{aligned}$$

Similarly when u is negative, we set $\alpha_i = x_{j-1/2} - (x_{i+1/2} - u\Delta t)$; then $-\Delta x \le \alpha_i \le 0$ and

$$\begin{aligned}\Phi_{i+1/2}(t^n) &= \int_{x_{j-1/2}-\alpha_i}^{x_{i+1/2}} f(t^n, x)\,dx \\ &= \Delta x \sum_{k=i+1}^{j-1} f_k + \alpha_i \Bigg[f_j - \frac{\epsilon_j^+}{6}\left(1 - \frac{\alpha_i}{\Delta x}\right)\left(1 + \frac{\alpha_i}{\Delta x}\right)(f_{j+1} - f_j) \\ &\quad + \frac{\epsilon_j^-}{6}\left(2 + \frac{\alpha_i}{\Delta x}\right)\left(1 + \frac{\alpha_i}{\Delta x}\right)(f_j - f_{j-1}) \Bigg].\end{aligned}$$

2.4. Discretization of Boundary Conditions

In order to complete our numerical method we must discuss the numerical treatment of the boundary conditions. We consider Eq. (1) supplemented with the boundary conditions

$$|v \cdot n| f(x, v, t) = \int_{v_* \cdot n < 0} |v_* \cdot n(x)| K(v_* \to v, x, t) f(x, v_*, t)\,dv_* \quad \text{for } v \cdot n \ge 0,\ x \in \partial\Omega. \tag{23}$$

The smooth boundary $\partial\Omega$ is assumed to have a unit inner normal $n(x)$ at every $x \in \partial\Omega$. The boundary condition (23) is the so-called reflective condition on $\partial\Omega$. The ingoing flux is defined in terms of the outgoing flux modified by a given boundary kernel K according to the integral in (23). This boundary kernel is such that positivity and mass conservation at the boundaries are guaranteed:

$$K(v_* \to v, x, t) \ge 0, \quad \int_{v \cdot n(x) \ge 0} K(v_* \to v, x, t)\,dv = 1. \tag{24}$$

From a physical point of view, we assume that at the solid boundary a fraction α of particles is absorbed by the wall and then reemitted with the velocities corresponding to those in a still plasma at the temperature of the solid wall, while the remaining portion $(1 - \alpha)$ is

perfectly reflected. This is equivalent to imposing for the ingoing velocities

$$f(x, v, t) = (1 - \alpha)Rf(x, v, t) + \alpha Mf(x, v, t), \quad x \in \partial\Omega, v \cdot n(x) \geq 0, \tag{25}$$

with $0 \leq \alpha \leq 1$, and

$$Rf(x, v, t) = f(x, v - 2n(n \cdot v), t), \tag{26}$$

$$Mf(x, v, t) = \mu(x, t) f_s(v). \tag{27}$$

In (27), if we denote Boltzmann's constant by k_B and the temperature of the solid boundary by T_s, f_s is given by

$$f_s(v) = 2\pi T_s M_{1,0,T_s}(v) = \exp\left(-\frac{v^2}{2k_B T_s}\right),$$

and the value of μ is determined by mass conservation at the surface of the wall:

$$2\pi T_s \mu(x, t) \int_{v\cdot n \geq 0} M_{1,0,T_s}(v)|v \cdot n|\, dv = \int_{v\cdot n<0} f(x, v, t)|v \cdot n|\, dv. \tag{28}$$

We point out that the discretization of specular reflection is obvious for simple geometries whereas it is more difficult for more complex geometries (for which the boundaries are not symmetry axes of the grid used for the discrete velocity distribution).

On the other hand the discretization of diffusive boundary conditions even for simple geometries is not obvious. For simplicity, we only present the scheme for a simple one-dimensional problem on the interval (x_{min}, x_{max}). Extension to multidimensional geometries with straight boundaries follows straightforwardly.

Assume the values of the distribution function at time t^n are known: $\{f_i^n\}_{i\in I}$. When the origin of the characteristic curve is inside the domain, the values at time t^{n+1} can be computed directly using the scheme for the internal points. In contrast, when the origin of the characteristic is outside the domain, for example at $x = x_{min}$, we compute $\mu^{n+1/2}(x_{min})$ as an approximation of $\mu(t, x_{min})$ on the interval $[t^n, t^{n+1}]$ by

$$2\pi T_s \int_{t^n}^{t^{n+1}} \mu(t, x_{min}) \int_{v\geq 0} M_{1,u_s,T_s}(v)\, v\, dv\, dt$$
$$= -\int_{t^n}^{t^{n+1}} \int_{v\leq 0} f(t, x_{min,} v)\, v\, dv\, dt.$$

For negative velocities the distribution function on $[t^n, t^{n+1}]$ is given from the characteristic curves

$$\frac{dX}{ds}(s) = v, \quad X(t) = x_{min},$$

and the solution at time t^n can be easily computed: $X(t^n, t, x_{min}) = x_{min} + v(t^n - t)$. Then

$$\begin{aligned} 2\pi T_s \int_{t^n}^{t^{n+1}} \mu(t, x_{min}) \int_{v\le 0} M_{1,0,T_s}(v)\, v\, dv\, dt \\ = -\int_{v\le 0} \int_{t^n}^{t^{n+1}} f(t^n, X(t^n, t, x_{min}), v)\, v\, dt\, dv \\ = -\int_{v\le 0} \int_{x_{min}}^{x_{min} - v\Delta t} f(t^n, x, v)\, dx\, dv. \end{aligned}$$

Finally, the value $\mu^{n+1/2}(x_{min})$ is computed as

$$\mu^{n+1/2}(x_{min}) = \frac{\int_{v\le 0} \int_{x_{min}}^{x_{min} - v\Delta t} f(t^n, x, v)\, dx\, dv}{2\pi T_s \Delta t \int_{v\ge 0} M_{1,0,T_s}(v)\, v\, dv}.$$

From the value $\mu^{n+1/2}$, we can approximate the flux of particles when the origin of the characteristic is outside the domain. For a positive velocity v_j, if we denote by $\bar{t} \in [t^n, t^{n+1}]$, such that $x_{min} = X(\bar{t}, t^{n+1}, x_{i+1/2})$, we have

$$\begin{aligned} \Phi_{i+1/2,j}(t^n) &= \int_{X(\bar{t}, t^{n+1}, x_{i+1/2})}^{x_{i+1/2}} f(t^n, x, v_j)\, dx + \int_{t^n}^{\bar{t}} f(t, x_{min}, v_j) v_j\, dt \\ &= \Delta x \sum_{k=0}^{i} f_{i,j}^n + (\bar{t} - t^n) \mu^{n+1/2}(x_{min}) M_{1,0,T_s}(v_j). \end{aligned}$$

3. NUMERICAL TESTS

3.1. Space Homogeneous Problems

Test 1: The Maxwellian case in 2D ($\gamma = 0$). The initial data is chosen on the class of known exact isotropic solutions which is an extension of Bobylev solutions for the Boltzmann equation in the case of Maxwell molecules [3]. Precisely we compare in two dimensions our numerical results with the exact solution

$$f(v, t) = \frac{1}{2\pi S}\left(1 - \frac{1 - S}{S}\left(1 - \frac{|v|^2}{2S}\right)\right) \exp\left(-\frac{|v|^2}{2S}\right),$$

where $S = 1 - 0.5\exp(-2t)$.

This test is carried out to compare the efficiency of the third-order DUMKA solver with the standard explicit Euler scheme. For more-complete accuracy tests we refer readers to [37]. The simulation is stopped at $t = 0.8$ when a stationary state is achieved which, for example, corresponds to the stabilization of the kinetic entropy (see Fig. 1). We use $n = 16$, 32, and 64 modes in each direction, whereas the time step Δt and the support of the distribution function depend on the size of the grid. The support of f is increased with the number of modes, and $v_{max} = 3\pi/4$, $9\pi/10$, and π for $n = 16^2$, 32^2, and 64^2 modes, respectively.

The total computation time and the different time steps used are reported in Table I with respect to the number of modes. It is evident that the DUMKA scheme allows larger time steps (5–10 times larger then Euler scheme) and permits a high reduction of the computation

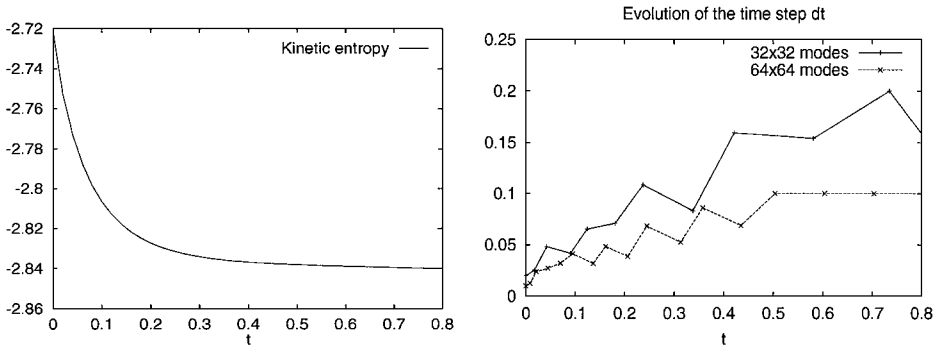

FIG. 1. (Test 1) Decay in time of the numerical entropy with $n = 32$ modes (left) and adaptive time stepping for the DUMKA scheme (right).

time when the number of unknowns is increased. Indeed, with 64^2 modes the third-order DUMKA scheme with adaptive time stepping is about four times faster than the simple Euler method.

The relative quadratic error norm is plotted in Fig. 2. For example at time $t = 0.1$ we observe that when passing from 16 to 32 modes the error decreases approximately by a factor of 10 for the Euler method, by a factor of 500 for the fixed DUMKA method, and by 250 for the variable DUMKA. The respective convergence rates are then 3.3, 9, and 8. Similarly when we pass from 32 to 64 we obtain the convergence rates of 3.1 for Euler and 6.7 and 8 for the DUMKA method. This shows that the DUMKA scheme permits as to keep the spectral accuracy without increasing the computational cost. Therefore, it is suitable for coupling in an efficient way the spectral method with the transport step.

Test 2: Sum of two Maxwellian distributions in 3D ($\gamma = -3$). Next we considered the three-dimensional Coulombian case. The initial data is now chosen as the sum of two Maxwellian functions,

$$f_0(v) = \frac{1}{2}\frac{5}{\left(2\pi v_{th}^2\right)^{2/3}}\left[\exp\left(-\frac{|v-v_1|^2}{2v_{th}^2}\right) + \exp\left(-\frac{|v-v_2|^2}{2v_{th}^2}\right)\right],$$

with $v_1 = (1.25, 1.25, 0)$ and $v_2 = (-1.25, -1.25, 0)$, and where the thermal velocity is $v_{th} = 0.4$. The final time of the simulation is $T_{end} = 80$. In Fig. 3 we report the evolution of

TABLE I
Total Computation Time for the Fixed-Time-Step Euler Scheme and for the DUMKA Scheme with Fixed and Variable Time Stepping (Test 1)

	Euler (fixed)		DUMKA (fixed)		DUMKA (variable)
Number of modes	CPU time	Δt	CPU time	Δt	CPU time
16×16	001.2	5.0e-3	001.6	2.50e-2	000.6
32×32	012.0	1.0e-3	013.0	1.25e-2	005.0
64×64	512.0	1.0e-4	515.0	1.00e-3	143.0

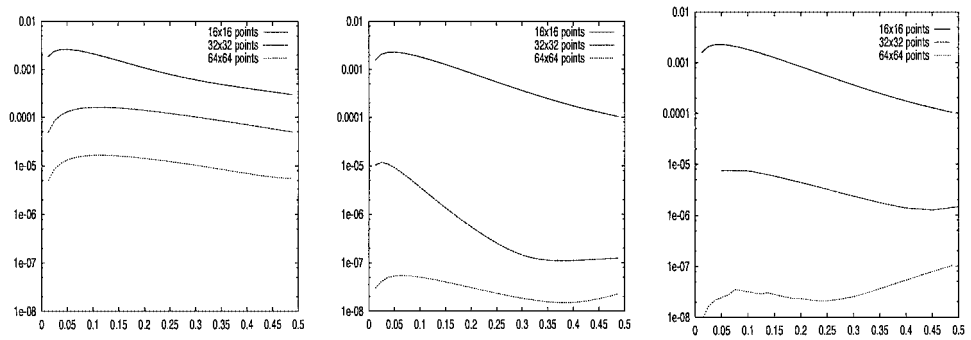

FIG. 2. (Test 1) Evolution of the relative quadratic error for the Euler scheme (left), and for the DUMKA scheme with fixed (middle) and variable (right) time steps using 16, 32, and 64 modes per direction.

the level set of the distribution function $f(t, v_x, v_y, v_x) = 0.02$ obtained with $n = 32$ modes at different times. Initially the level set of the initial data corresponds to two "spheres" in the velocity space. Then, the two distributions start to mix together until the stationary state is reached, represented by a single centered sphere. It is clear that the spherical shapes of the level sets are described with great accuracy by the spectral method.

3.2. Space Nonhomogeneous Problems

Test 3: Landau damping. We now consider the one-dimensional Vlasov–Poisson equation coupled with the two-dimensional FPL collision operator

$$\frac{\partial f}{\partial t} + v_x \frac{\partial f}{\partial x} + E(t, x)\nabla_v f = \frac{1}{\epsilon} Q(f, f), \quad x \in \mathbb{R}, v \in \mathbb{R}^2, \tag{29}$$

where

$$E(t, x) = -\frac{\partial \phi(t, x)}{\partial x}, \quad -\frac{\partial^2 \phi(t, x)}{\partial x^2} = \int_{\mathbb{R}^2} f(t, x, v)\, dv - 1. \tag{30}$$

The initial data is

$$f(0, x, v_x, v_y) = \frac{1}{2\pi\sigma^2} \mathrm{e}^{-(v_x^2+v_y^2)/2\sigma^2}(1 + \alpha \cos(k\, x)), \quad \forall (x, v_x, v_y) \in (0, L) \times \mathbb{R}^2,$$

where $\sigma = 0.24$, $\alpha = 0.5$, $k = 2\pi/L$, and $L = 4$. The boundary conditions are assumed to be periodic in space. Without collision, the Vlasov equation develops thin filaments in phase space and steep gradients in v are generated. Therefore, a large number of points in the velocity space are necessary to discretize the Vlasov equation in the transport step. We use a number of cells $N_x = 32$ in the x-direction and $N_{v_x} = N_{v_y} = 64$ in the v-direction. On the other hand, the FPL equation acts on large scales and the computational cost of the collision operator is strongly increased when the number of unknowns is increased; therefore a coarser grid with $N_{v_x} = N_{v_y} = 32$ is used in the collision phase. This can be justified from the fact that the scheme is spectrally accurate in velocity for the collision step, but less accurate for the transport step, and therefore a smaller grid is required by the latter in order to match the accuracy of the collision step.

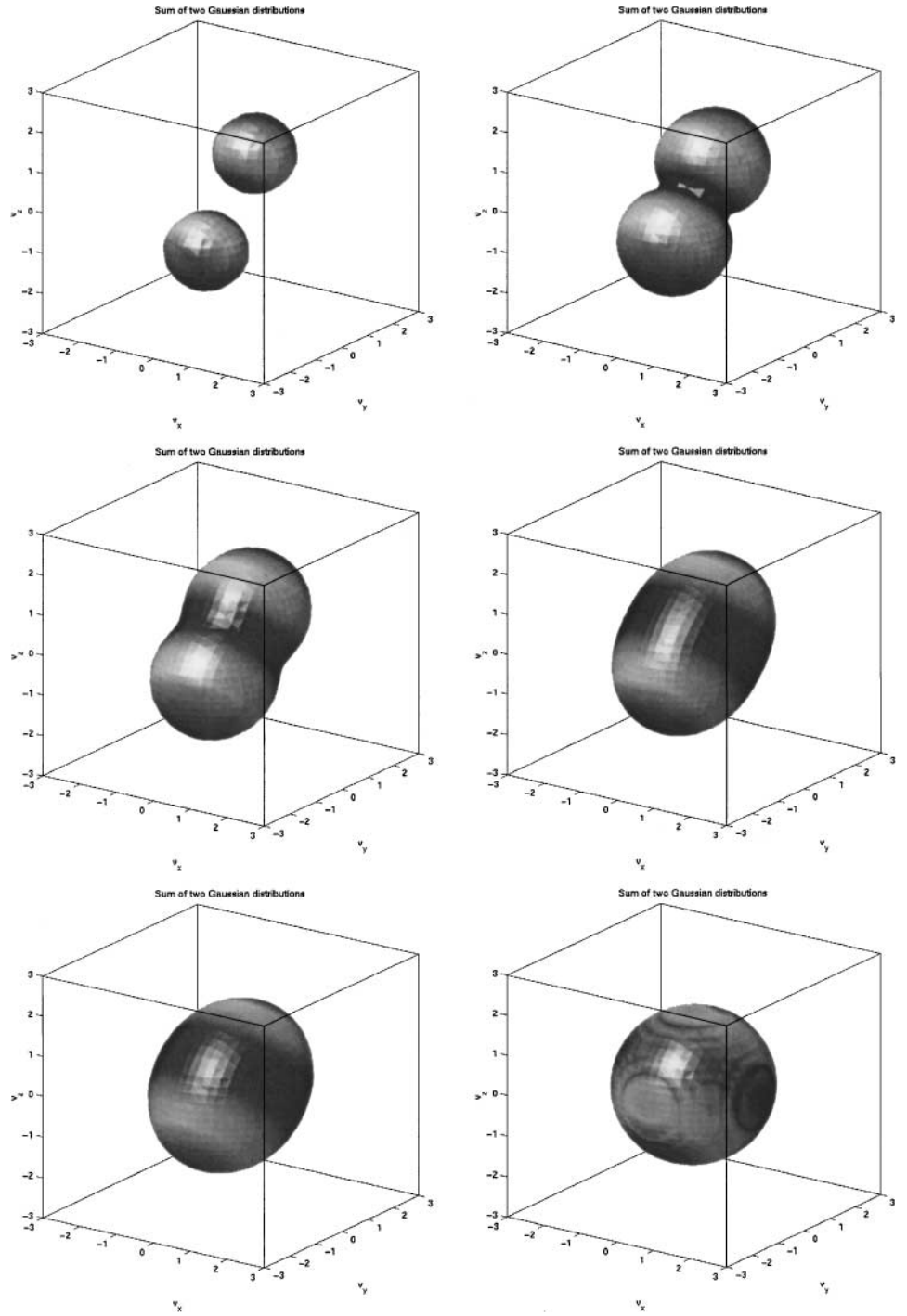

FIG. 3. (Test 2) Evolution of the level set $f(t, v_x, v_y, v_x) = 0.02$ with $n = 32$ modes in the Coulombian case at times $t = 0, 7.5, 12.5, 27.5, 37.5, 77.5$.

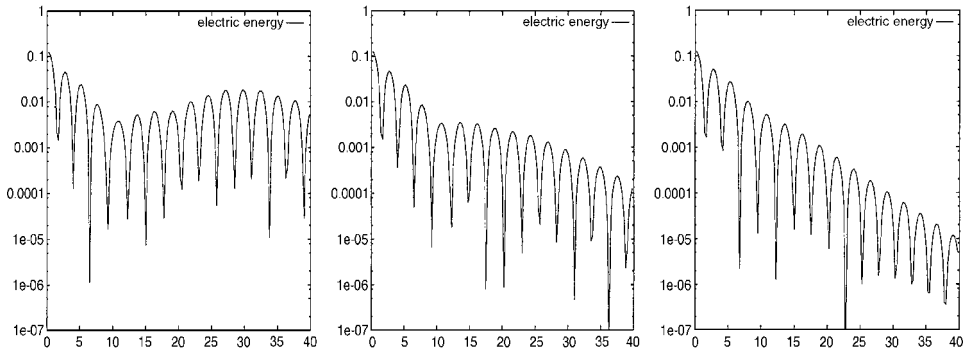

FIG. 4. (Test 3) Time evolution of the electric energy in logarithmic scale with respect to the Knudsen number; $\epsilon = +\infty$ (left), $\epsilon = 200$ (middle), and $\epsilon = 50$ (right).

The two velocity grids are linked using the natural trigonometric interpolation derived from the Fourier representation. This allows the use of the same time step for transport and collisions.

The evolution of the discrete electric energy,

$$\sum_i \Delta x E_i^2(t), \quad E_i(t) = E(t, x_i),$$

in logarithmic scale is plotted in Fig. 4 with respect to the Knudsen number ε. In practice the time evolution consists of rapid oscillations around a slowly varying average, where the average is taken over an oscillation period. The value $\varepsilon = +\infty$ corresponds to the Vlasov–Poisson system without Coulombian interactions between particles. In this case the electric energy is first exponentially decreased and next starts to oscillate around a constant value. At variance, in the presence of collisions, the electric energy is still decreasing in time. Moreover, when the collision frequency is strong enough, it continues to decrease exponentially. Concerning the evolution of the distribution function in the (x, v_x) space, without collision, the variations of the electric energy create small bumps (that need to be resolved in the velocity space) around the phase velocity $v_\phi = \omega/k$, where ω is the oscillation frequency and k is the wave number. But when collisions are taken into account, the Landau operator acts as a diffusion equation and the oscillations generated by the coupling with the Poisson equation are dumped and the stationary state holds early. We report in Figs. 5 and 6 (respectively) the results for

$$F(t, v_x) = \int_{\mathbb{R}\times\mathbb{R}} f(t, x, v_x, v_y)\, dx\, dv_y, \quad F_y(t, x, v_x) = \int_{\mathbb{R}} f(t, x, v_x, v_y)\, dv_y.$$

Test 4: Wave reflection. In the last test problem, we consider the Landau equation in the absence of external forces ($E \equiv 0$) in the four-dimensional phase space, $\Omega \times \mathbb{R}^2$, where $\Omega = (0, 1) \times (0, 1)$. The equation reads

$$\frac{\partial f}{\partial t} + v_x \frac{\partial f}{\partial x} + v_y \frac{\partial f}{\partial y} = \frac{1}{\varepsilon} Q(f, f), \quad (x, y) \in \Omega, \quad (v_x, v_y) \in \mathbb{R}^2, \tag{31}$$

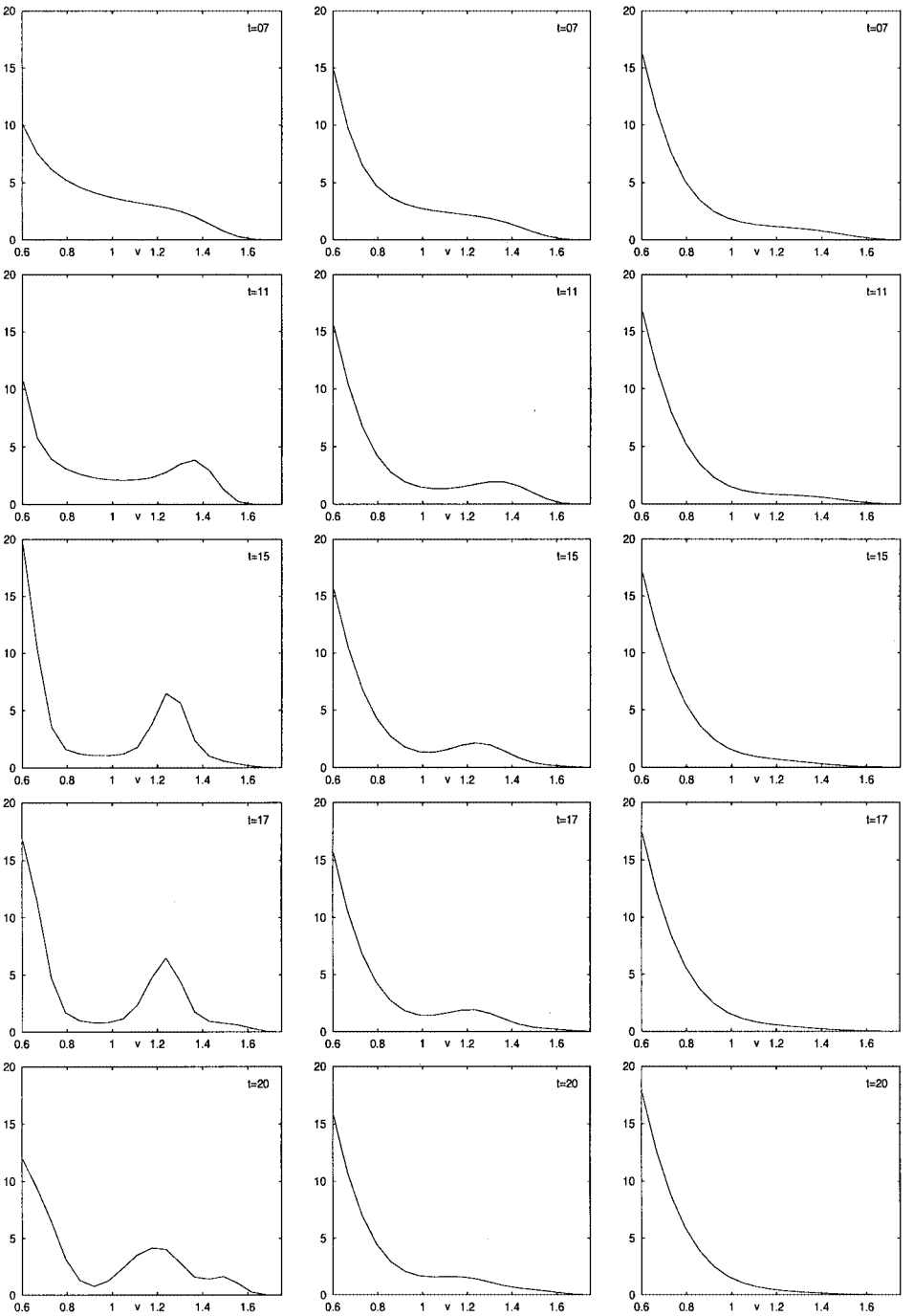

FIG. 5. (Test 3) Time evolution of the tail of the (x, v_y)-integrated distribution function with respect to the Knudsen number; $\epsilon = +\infty$ (left), $\epsilon = 200$ (middle), and $\epsilon = 50$ (right).

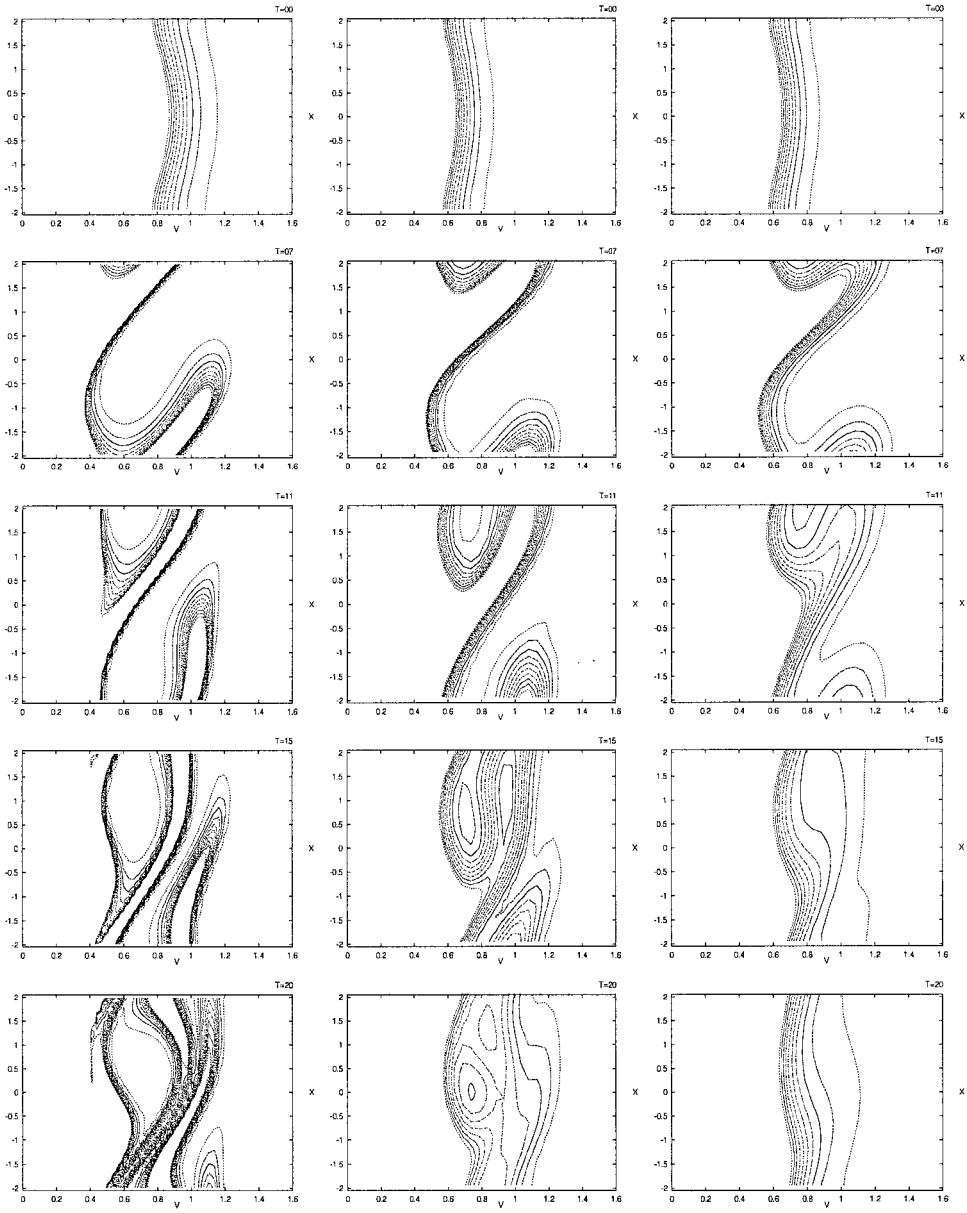

FIG. 6. (Test 3) Time evolution in phase space of the v_y-integrated distribution function with respect to the Knudsen number; $\epsilon = +\infty$ (left), $\epsilon = 200$ (middle), and $\epsilon = 50$ (right).

with the boundary condition

$$f(t, x, y, v) = \mu(t)\ \exp(-v^2/\sigma_w(x, y)), \quad (x, y) \in \partial\Omega, v \cdot n \leq 0, \tag{32}$$

where n is the outer normal at the boundary. The value $\mu(t)$ is computed such that the number of particles is conserved, and $\sigma_w(x, y)$ represents the temperature of the wall and

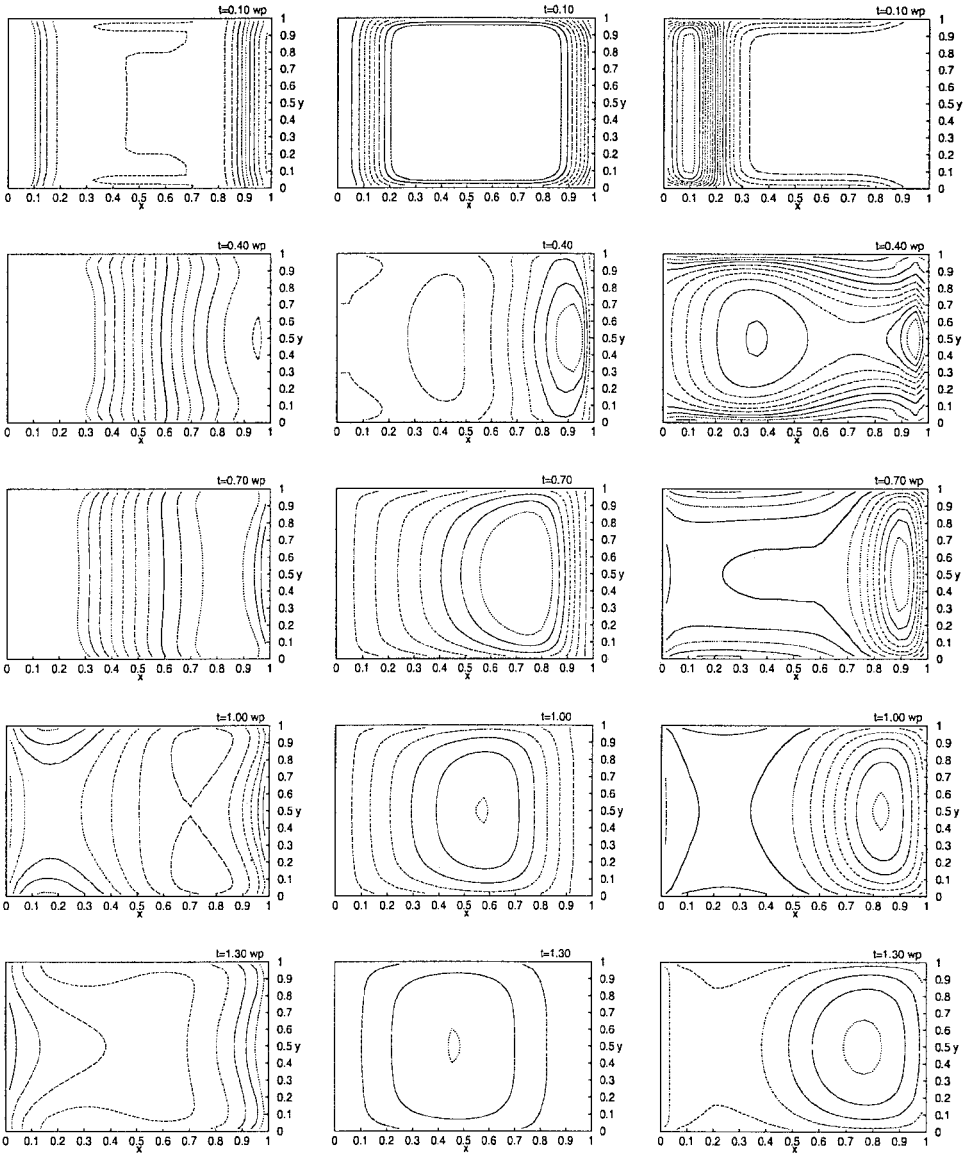

FIG. 7. (Test 4) Time evolution of the density (left), the x-component of the mean velocity (middle), and temperature (right) for $\varepsilon = 1$.

is given by

$$\sigma_w(x, y) = \begin{cases} 3\sigma & \text{if } x = 0,\ y \in (0, 1), \\ \sigma & \text{elsewhere,} \end{cases}$$

with $\sigma = 0.25$.

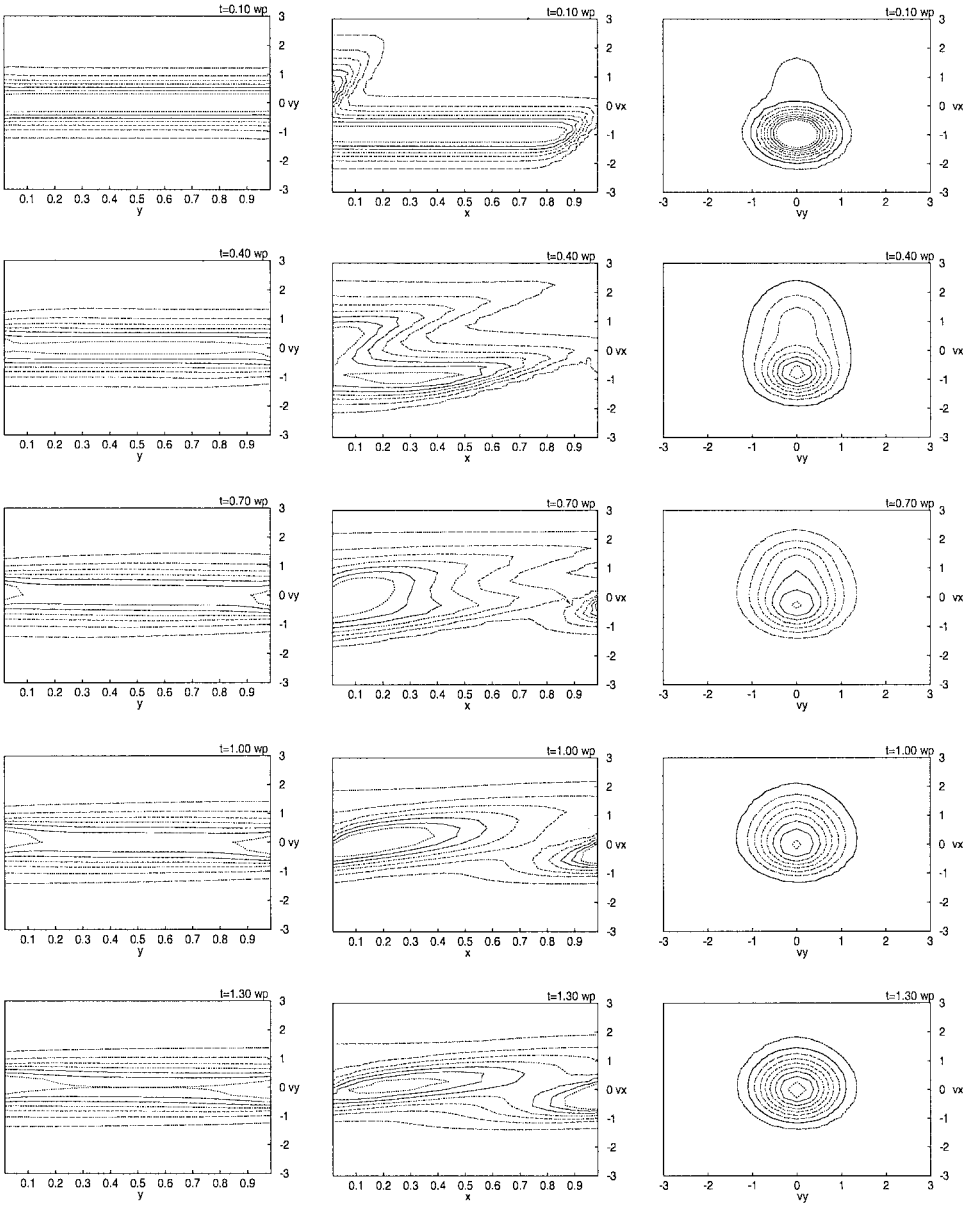

FIG. 8. (Test 4) Time evolution of the (x, v_x)-integrated (left), (y, v_y)-integrated (middle), and (x, y)-integrated (right) distribution function for $\varepsilon = 1$.

The initial data is chosen as

$$f_0(x, y, v) = \frac{1}{2\pi\sigma} \exp\left(-\left(\frac{(v_x + 1)^2 + v_y^2}{2\sigma}\right)\right),$$

so that the total mean velocity is $u(x, y) = (-1, 0)$ and the initial temperature is constant, $T(x, y) = 1/2$.

We consider the evolution of the density ρ, mean velocity u, and temperature T of the plasma and of the quantities

$$F_y(t, x, v_x) = \int_{[0,1]\times\mathbb{R}} f(t, x, y, v)\, dv_y\, dy,$$

$$F_x(t, y, v_y) = \int_{[0,1]\times\mathbb{R}} f(t, x, y, v)\, dv_x\, dx,$$

$$F(t, v) = \int_{\Omega} f(t, x, y, v)\, dx\, dy.$$

We present results for $\varepsilon = 1$. The number of cells on Ω is $N_x = 64$ and $N_y = 32$ and a 32×32 velocity grid for both transport and collision has been used. Thanks to the absence of forces the ratio between the collisional and the transport time steps can be kept to one. Figure 7 shows the contour plots of density, mean velocity, and temperature. The front of the mean velocity and temperature moves along the x-axis and is reflected by the boundary $x = 1$. The values of the integrated distribution functions F_x, F_y, and F are reported in Fig. 8. The distribution function is initially a Maxwellian centered at $u = (-1, 0)$ which evolves until the stationary state is centered in $u_e = (0, 0)$ with a different temperature. The (y, v_y)-integrated distribution function shows that for transient times when transport dominates collisions, steep gradients on the velocity space are generated and a large number of points are necessary to accurately describe the distribution function.

4. CONCLUSION

We have presented an efficient and accurate numerical method to solve the FPL equation in space nonhomogeneous situations. The collision operator is solved in only $O(N \log_2 N)$ operations using a spectral method based on approximating the distribution function by a partial sum of Fourier series. The scheme conserves mass and approximates momentum and energy with spectral accuracy provided a sufficiently large support in the velocity space is used. For the time discretization a scheme with a large stability region is needed to overcome the diffusive stiffness of the collision operator. To this aim two different techniques have been developed: a high-order explicit Runge–Kutta method with a large stability region and different grids in velocity space during transport and collisions. This approach highly improves the efficiency of the method and seems to be a good compromise between accuracy and computational cost. Finally the transport has been solved with an accurate flux conservative method and different kinds of boundary conditions have been discussed and implemented.

REFERENCES

1. A. A. Arsen'ev and O. E. Buryak, On the connection between a solution of the Boltzmann equation and a solution of the Fokker–Planck–Landau equation, *Math. USSR Sbornik* **69**, 465 (1991).
2. Yu. A. Berezin, V. N. Khudick, and M. S. Pekker, Conservative finite difference schemes for the Fokker-Planck equation not violating the law of an increasing entropy, *J. Comput. Phys.* **69**, 163 (1987).
3. A. V. Bobylev, Exact solutions of the Boltzmann equation, *Dokl. Akad. Nauk. S.S.S.R.* **225**, 1296 (1975) (Russian).
4. A. V. Bobylev and K. Nanbu, Theory of collision algorithms for gases and plasmas based on the Boltzmann equation and the Landau–Fokker–Planck equation, *Phys. Rev. E* **61**(4), 4576 (2000).

5. A. V. Bobylev, I. F. Potapenko, and V. A. Chuyanov, Completely conservative difference schemes for nonlinear kinetic equation of Landau (Fokker–Planck) type, *Akad. Nauk SSSR Inst. Prikl. Mat. Preprint* **76**, 26 pp. (1980) (Russian).
6. A. V. Bobylev and S. Rijasanow, Difference scheme for the Boltzmann equation based on the Fast Fourier Transform, *Eur. J. Mech. B Fluids* **16**(2) 293 (1997).
7. C. Buet and S. Cordier, Numerical analysis of conservatives and entropy schemes for the Fokker–Planck–Landau equation, *SIAM J. Numer. Anal.* **36**(3), 953 (1999).
8. C. Buet and S. Cordier, Conservative and entropy decaying numerical scheme for the isotropic Fokker–Planck–Landau equation, *J. Comput. Phys.* **145**, 228 (1998).
9. C. Buet, S. Cordier, P. Degond, and M. Lemou, Fast algorithms for numerical, conservative, and entropy approximations of the Fokker-Planck equation, *J. Comput. Phys.* **133**, 310 (1997).
10. C. Buet, S. Cordier, and F. Filbet, Comparison of numerical schemes for Fokker–Planck–Landau equation, *ESAIM Proc.* **10**, 161 (2001).
11. M. G. Cadjan and M. F. Ivanov, Simulation of the collisional plasma kinetics under the action of laser and particle beams, *ICPP 25th Conf. Contr. Fusion Plasma Phys. ECA* **22C** 1047 (1998).
12. C. Canuto, M. Y. Hussaini, A. Quarteroni, and T. A. Zang, *Spectral Methods in Fluid Dynamics* (Springer-Verlag, New York, 1988).
13. C. Cercignani, *The Boltzmann Equation and Its Applications* (Springer-Verlag, Berlin, 1988).
14. C. Cercignani, R. Illenr, and M. Pulvirenti, *The mathematical Theory of Dilute Gases* (Springer-Verlag, New York, 1995).
15. J. S. Chang and G. Cooper, A practical difference scheme for Fokker–Planck equations, *J. Comput. Phys.* **6**, 1 (1970).
16. P. Degond and B. Lucquin-Desreux, The Fokker–Planck asymptotics of the Boltzmann collision operator in the Coulomb case, *Mathematical Models and Methods in the Applied Sciences* **2**, 167 (1992).
17. P. Degond and B. Lucquin-Desreux, An entropy scheme for the Fokker–Planck collision operator of plasma kinetic theory, *Numer. Math.* **68**, 239 (1994).
18. L. Desvillettes, On asymptotics of the Boltzmann equation when the collisions become grazing, *Transp. Theory Stat. Phys.* **21**, 259 (1992).
19. L. Desvillettes and C. Villani, On the spatially homogeneous Landau equation for hard potentials. Part I: Existence, uniqueness and smoothness; Part II: H-theorem and applications, *Commun. PDE* **25**(1-2), 179 (2000).
20. Yu. N. Dnestrovsij and D. P. Kostomarov, *Numerical Simulations of Plasmas* (Springer-Verlag, Berlin, 1986).
21. E. M. Epperlein, Implicit and conservative difference schemes for the Fokker–Planck equation, *J. Comput. Phys.* **112**, 291 (1994).
22. E. Fijalkow, A numerical solution to the Vlasov equation, *Comput. Phys. Commun.* **116**, 319 (1999).
23. D. Gottlieb and S. A. Orszag, *Numerical Analysis of Spectral Methods: Theory and Applications* SIAM CBMS-NSF Series (Soc. for Industr. & Appl. Math., Philadelphia, 1977).
24. I. K. Khabibrakhmanov and G. V. Khazanov, The spectral collocation method for the kinetic equation with the nonlinear two-dimensional coulomb collisional operator, *J. Comput. Phys.* **161**, 558.
25. L. D. Landau, Die kinetische gleichung für den fall Coulombscher vechselwirkung, *Phys. Z. Sowjet.* 154 (1936); translated in *The Transport Equation in the Case of the Coulomb Interaction*, Collected papers of L. D. Landau, edited by D. ter Haar (Pergamon, Oxford, UK (1981), p. 163.
26. M. Lemou, Multipole expansions for the Fokker–Planck–Landau operator, *Numer. Math.* **78**, 597 (1998).
27. E. W. Larsen, C. D. Levermore, G. C. Pomraning, and J. G. Sanderson, Discretization methods for one dimensional Fokker–Planck operators, *J. Comput. Phys.* **61**, 359 (1985).
28. V. I. Lebedev, *How to Solve Stiff Systems of Differential Equations by Explicit Methods; Numerical Methods and Applications* (CRC, Boca Raton, FL, 1994).
29. B. Lucquin-Desreux, Discrétization de l'opérateur de Fokker–Planck dans le cas homogène, *C. R. Acad. Sci. Paris* **314**, 407 (1992).
30. A. A. Medovikov, High order explicit methods for parabolic equations, *BIT* **38**(2), 372 (1998).

31. V. A. Mousseau and D. A. Knoll, Fully Implicit Kinetic Solution of Collisional Plasmas, *J. Comput. Phys.* **136**, 308.
32. K. Nanbu and S. Yonemura, Weighted particles in Coulomb collision simulations based on the theory of a cumulative scattering angle, *J. Comput. Phys.* **145**, 639 (1998).
33. T. Ohwada, Higher order approximation methods for the Boltzmann equation, *J. Comput. Phys.* **139**, 1 (1998).
34. L. Pareschi and B. Perthame, A Fourier spectral method for homogeneous Boltzmann equations, *Transp. Theory Stat. Phys.* **25**, 369 (1996).
35. L. Pareschi and G. Russo, Numerical solution of the Boltzmann equation. I: Spectrally accurate approximation of the collision operator, *SIAM J. Numer. Anal.* **37**, 1217 (2000).
36. L. Pareschi and G. Russo, On the stability of spectral methods for the homogeneous Boltzmann equation, *Transp. Theory Stat. Phys.* **29**, 431 (2000).
37. L. Pareschi, G. Russo, and G. Toscani, Méthode spéctrale rapide pour l'equation de Fokker–Planck–Landau, *C.R. Acad. Sci.* **1**, 517 (2000).
38. L. Pareschi, G. Russo, and G. Toscani, Fast spectral methods for the Fokker–Planck–Landau collision operator, *J. Comput. Phys.* **165**, 1 (2000).
39. L. Pareschi, G. Toscani, and C. Villani, Spectral methods for the non cut-off Boltzmann equation and numerical grazing collision limit, preprint (1999).
40. M. S. Pekker and V. N. Khudik, Conservative difference schemes for the Fokker–Planck equation. *U.S.S.R. Comput. Math. Math. Phys.* **24**(3), 206 (1984).
41. I. F. Potapenko and C. A. de Arzevedo, The completely conservative difference schemes for the nonlinear Landau–Fokker–Planck equation, *J. Comput. Appl. Math.* **103**, 115 (1999).
42. J. Qiang, R. D. Ryne, and S. Habib, Self-consisten Langevin simulation of Coulomb collisions in charged particle beams, *IEEE Trans.* 1 (2000).
43. M. N. Rosenbluth, W. MacDonald, and D. L. Judd, Fokker–Planck equation for an inverse square force, *Phys. Rev.* **107**, 1 (1957).
44. E. Sonnendrücker, J. Roche, P. Bertrand, and A. Ghizzo, The semi-Lagrangian method for the numerical resolution of Vlasov equations. *J. Comput. Phys.* **149**, 201 (1998).
45. G. Strang, On the construction and comparison of difference schemes, *SIAM J. Numer. Anal.* **5**, 506 (1968).
46. F. S. Zaitsev, V. V. Longinov, M. R. O Brien, and R. Tunner, Difference schemes for the time evolution of three-dimensional kinetic equations, *J. Comput. Phys.* **147**, 239 (1998).
47. C. Villani, A review of mathematical topics in collisional kinetic theory, in *Handbook of Fluid Mechanics*, edited by S. Frielander and D. Serre, to appear.